Comparison of potential calculations with helium diffraction and thermal desorption data of CF_4 and CF_3Cl adsorbed on Cu(110)

A. Marmier and C. Girardet
Laboratoire de Physique Moléculaire, UMR CNRS 6624, Faculté des Sciences La Bouloie, Université de Franche-Comté, 25030 Besançon Cedex, France

V. Diercks, R. David, and P. Zeppenfeld*
Institut für Grenzflächenforschung und Vakuumphysik, Forschungszentrum Jülich GmbH, 52425 Jülich, Germany
(Received 16 September 1997)

Helium atom scattering and thermal desorption spectroscopy are used to determine the adsorption properties of the tetrahedral and pyramidal molecules CF_4 and CF_3Cl, respectively, on the Cu(110) surface. High-order commensurate structures with large unit cells are obtained for CF_4 and CF_3Cl. The thermal desorption spectra reveal a zero-order desorption process for both species. A ''leading edge'' analysis yields monolayer adsorption energies of 161 ± 6 meV for CF_4 and 260 ± 6 meV for CF_3Cl. Semiempirical potential calculations corroborate these values and show that the shape of the potential energy maps for the two molecules is not very different, leading to tripod-down equilibrium configurations. The calculations also indicate some trends for an orientationally ordered structure for CF_3Cl along the Cu troughs which could be at the origin of a ferroelectric phase. [S0163-1829(98)05235-7]

I. INTRODUCTION

In contrast to the large body of work devoted to the adsorption of small spherical and linear molecules on various substrates, the studies of tetrahedral and pyramidal shape molecules are essentially restricted to methane and ammonia adsorbed on metals and dielectrics.[1] Heavier tetrahedral molecules have been studied in a more sporadic way. One example is CF_4 adsorbed on graphite (0001), which has been studied both in theory[2,3] and experiment.[4] As a result of the theoretical investigation of the phase diagram based either on equilibrium calculations of geometries,[2] or on molecular-dynamics simulations,[3] the CF_4 adlayer adopts rather complex structures as a function of coverage and surface temperature. The equilibrium site for the single admolecule was found to be on top of the carbon atom with a tripod-down configuration (with the three fluorine atoms pointing towards the surface). Another case is the adsorption of pyramidal CF_3Cl molecules on graphite, which has been studied mainly by x-ray diffraction.[5] The coverage-temperature phase diagram revealed three crystalline phases in the submonolayer regime: incommensurate, commensurate, and high-order commensurate structures, the latter corresponding to a ferroelectric arrangement of CF_3Cl chains. A single molecule adsorbed on graphite was shown[6] to be preferentially adsorbed on a site that is slightly shifted away from the a top site, the chlorine atom being in general closest to the graphite substrate.

Recently, a series of experiments[7] has been conducted to investigate the structure and the thermodynamics of CF_4 adsorbed on the Cu(110) surface. The occurrence of high-order commensurate phases ($n\times18; n\simeq13$, and $n=2$), corroborated the fact that this type of molecule generally forms complex two-dimensional structures on corrugated substrates. Semiempirical potential calculations[8] showed that it is quite difficult to interpret these structures on the basis of numerical energy minimization procedures. Indeed, the stable geometry is probably the result of a subtle energy balance between positional and orientational ordering of the molecules on the surface. This ordering arises from a competition between the surface corrugation of the Cu(110) substrate, which tends to favor sites inside the potential throughs along the $[1\bar{1}0]$ direction and the lateral interactions, which impose specific distances and orientations between the tetrahedral molecules. The resulting adlayer geometry is a crooked configuration of the molecules on the corrugated substrate.[8] A logical extension of this study is to consider chlorine-substituted methane species. In this way, the weakly octupolar tetrahedral CF_4 molecule is transformed, in the present case, into a strongly dipolar pyramidal CF_3Cl molecule.

Thermal helium atom diffraction has been used to determine the geometry of the unit cell of the CF_3Cl monolayer within the same temperature and coverage range as for CF_4. In addition, thermal desorption spectroscopy (TDS) is employed to measure and compare the desorption energies for the two molecular species CF_4 and CF_3Cl in the monolayer and multilayer regime. Simultaneously, we have performed potential calculations to interpret these results.

In Sec. II, we present the experimental data on the structure and the desorption kinetics of CF_4 and CF_3Cl adlayers on Cu(110). In Sec. III we use semiempirical potentials to study the adsorption of CF_3Cl on the Cu(110) surface as we did for CF_4, Xe, and N_2 in previous papers.[8–10] We first discuss the potential parameters and determine the potential energy maps for single CF_4 and CF_3Cl molecules adsorbed on Cu(110). Next, we calculate the stable geometries of a hypothetical two-dimensional CF_3Cl layer without support and, finally, the molecular arrangement for selected superstructures including the contribution of the Cu(110) substrate. In Sec. IV, we compare the adsorption energies for the

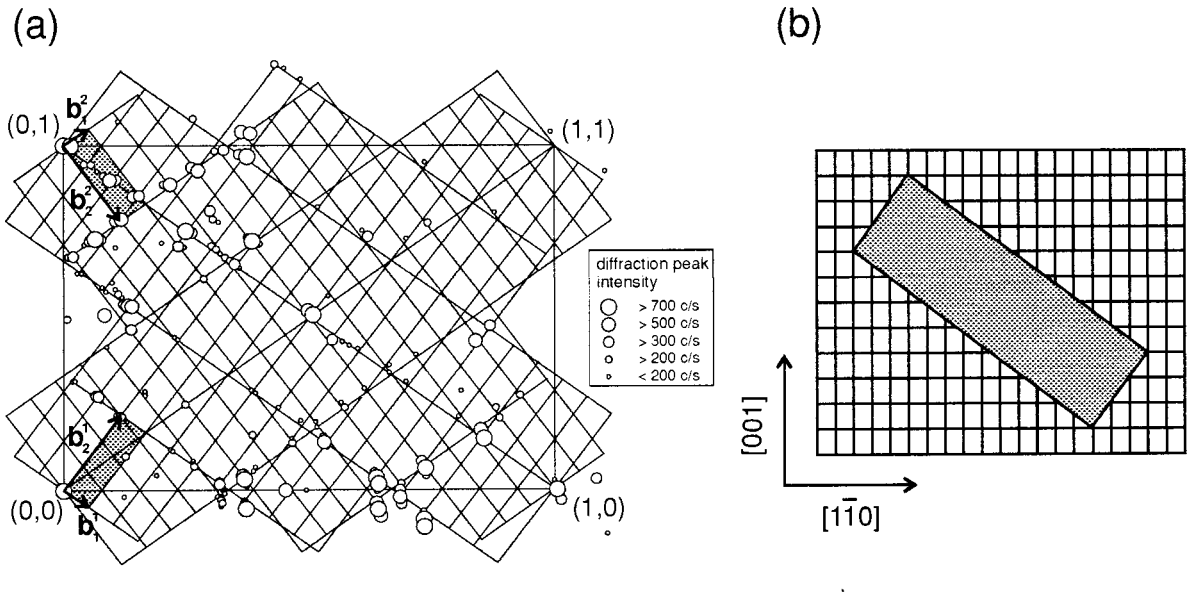

FIG. 1. (a) CF_3Cl unit cells (dark rectangles) for the two equivalent domains in reciprocal space and (b) the $\binom{13\ -7}{3\ \ 3}$ superstructure unit cell in real space.

two molecular species with the TDS data and discuss the adlayer geometries by comparing with available numerical and experimental data for CF_4 and CF_3Cl adsorbed on graphite.

II. EXPERIMENTAL DATA

A. Structure of monolayer CF_3Cl on Cu(110)

The structure of monolayer CF_3Cl adsorbed on the single crystal Cu(110) surface has been studied using thermal energy helium atom diffraction. The experimental setup is described in detail in Ref. 11. CF_3Cl was adsorbed by exposing the Cu(110) surface at 60 K to a partial pressure of CF_3Cl gas. The coverage was controlled by monitoring the specularly reflected helium intensity. The adlayer was then cooled down slowly to 20 K where the diffraction data were recorded.

The adlayer structure was characterized by so-called ''polar diffraction scans,'' in which the diffracted He intensity is recorded as a function of the parallel wave vector transfer at fixed azimuthal orientation of the sample. Figure 1(a) shows all the diffraction features that were extracted from the polar diffraction scans for a large number of azimuthal angles. The open circles indicate the peak positions with respect to the Cu(110) unit cell. The size of the circles is chosen according to the peak intensities after background subtraction. The diffraction spectra were always reproducible in several experiments, but the existence of metastable structures as observed for Xe/Cu(110) (Ref. 12) cannot be completely ruled out. A systematic study to map out the complete phase diagram for the CF_3Cl monolayer and to determine the stability of the adlayer structure was not performed.

The diffraction spectra reveal a large number of peaks, the majority of which can be assigned to the two grids drawn in Fig. 1(a). Obviously, the corresponding unit cells [shaded areas in Fig. 1(a)] characterize the two (symmetrically equivalent) domains of the superstructure of the CF_3Cl monolayer. The unit vectors $\mathbf{b}_1^{1,2}$ and $\mathbf{b}_2^{1,2}$ of the two almost rectangular reciprocal unit cells can be expressed in terms of the Cu(110) reciprocal unit vectors $\mathbf{b}_1^{Cu}$ and $\mathbf{b}_2^{Cu}$ as

$$\mathbf{b}_1^{1,2}=\frac{1}{20}\mathbf{b}_1^{Cu}\mp\frac{1}{20}\mathbf{b}_2^{Cu}, \tag{1}$$

$$\mathbf{b}_2^{1,2}=\frac{7}{60}\mathbf{b}_1^{Cu}\pm\frac{13}{60}\mathbf{b}_2^{Cu}. \tag{2}$$

Equation (2) follows from the fact that the diagonals of the unit cells are

$$\mathbf{b}_1^{1,2}+\mathbf{b}_2^{1,2}=\frac{1}{6}\mathbf{b}_1^{Cu}\pm\frac{1}{6}\mathbf{b}_2^{Cu}.$$

By back transformation of the reciprocal unit cell into real space the CF_3Cl monolayer is found to have an oblique, high-order commensurate (HOC) $\binom{13\ -7}{3\ \ 3}$ structure on Cu(110). The lengths of the unit vectors are 41.7 and 13.3 Å, respectively, and the enclosed angle is about 91.2°. The corresponding unit cell is exactly 60 times the size of the Cu(110) unit cell [Fig. 1(b)]. Since the scattering of He atoms cannot be described by simple kinematic theory a straightforward interpretation of the peak intensities in terms of the arrangement and orientation of the CF_3Cl molecules inside the unit cell is not possible. On the other hand, any more sophisticated scattering calculation is not practicable for such complicated structures.

The structure of CF_4 on Cu(110) has been studied as well. The experimental results are described in Ref. 7 and compared to potential energy calculations in Ref. 8. In the submonolayer range a HOC (13×18) phase is observed, which converts into a (2×18) structure for coverages above one monolayer.

B. Thermal desorption spectroscopy (TDS)

The thermodynamics and the desorption kinetics of weakly bound adlayers can be investigated in detail and with

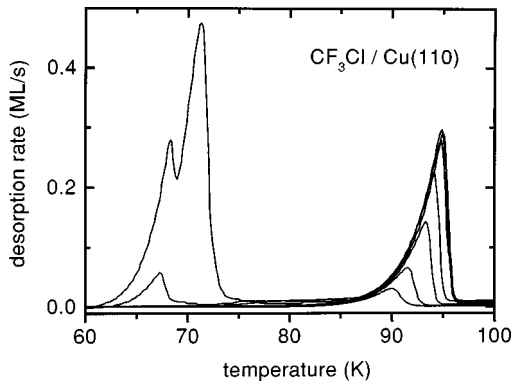

FIG. 2. Thermal desorption spectra of CF_3Cl from Cu(110) (heating rate: 1K/s) for seven different coverages ranging from 0.12 to 3.0 ML. Three peaks are observed, which can be assigned to desorption: the monolayer (260 ± 6 meV), bilayer (237 ± 6 meV), and multilayer (204 ± 6 meV).

high precision using TDS. After exposure of the crystal to a given coverage the crystal is heated with a constant heating rate. Simultaneously, the partial pressure of the desorbing species is measured in front of the surface by means of a quadrupole mass analyzer (QMA). For a sufficiently large pumping speed this partial pressure is proportional to the desorption rate[13] and the integrated QMA signal is a direct measure of the initial coverage. Scaling the QMA intensity to the integrated signal corresponding to one monolayer yields the desorption rate in units of monolayers per second (ML/s) as used in Figs. 2 and 3.

The temperature dependence of the desorption rate ν can be described by the Polanyi-Wigner equation[14,15]

$$\nu=-\frac{dn}{dt}=n^m k_0 \exp\left(-\frac{E_A}{k_B T}\right), \tag{3}$$

where t denotes the time, T the substrate temperature, n the number of adsorbed particles on the surface, m the order of desorption, E_A the adsorption or activation energy, k_0 the preexponential factor or attempt frequency, and k_B the Boltzmann constant.

Figures 2 and 3 show TDS spectra for different initial coverages from submonolayer to multilayer amounts of CF_3Cl and CF_4, respectively, using a heating rate of 1 K/s. For CF_3Cl, one can distinguish three different desorption peaks with increasing coverage, according to desorption of the monolayer, bilayer, and multilayer. The low temperature rises (leading edges) of the monolayer and the bilayer desorption peaks are the same for different CF_3Cl initial coverages. Hence, the number of particles participating in the desorption process at a given temperature is independent of their total number. According to Eq. (3), this corresponds to zero-order desorption ($m=0$). In this case the adsorption energy E_A can be determined from the slope of an Arrhenius plot, in which the QMA signal is plotted logarithmically as a function of the reciprocal surface temperature [as shown in Fig. 3(b) for the case of CF_4]:[13]

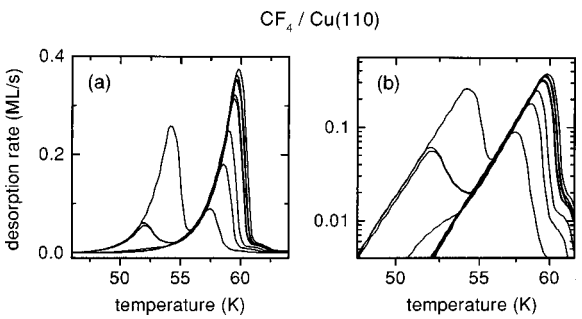

FIG. 3. Thermal desorption spectra of CF_4 from Cu(110) (heating rate: 1K/s) for nine different coverages ranging from 0.26 to 1.64 ML. A monolayer (161 ± 6 meV) and a bilayer (151 ± 6 meV) desorption peak can be distinguished. (a) Linear scale, (b) Arrhenius plot.

$$E_A=-\frac{1}{k_B}\frac{\partial \ln \nu}{\partial(1/T)}. \tag{4}$$

We have determined the adsorption energies for CF_3Cl to be 260 ± 6 meV for the monolayer, 237 ± 6 meV for the bilayer, and 204 ± 6 meV for the multilayer.

Whereas for CF_3Cl there is still a sizable difference between the adsorption energies of the bilayer and the multilayer, only two desorption peaks were observed for CF_4 (Fig. 3), indicating that the difference of the adsorption energies for the second and higher layers is quite small. The monolayer and multilayer peaks are both characteristic of zero-order desorption. The adsorption energies deduced from a leading edge analysis [Fig. 3(b)] are 161 ± 6 meV for monolayer and 151 ± 6 meV for multilayer CF_4, respectively. The monolayer energy is in good agreement with the value of the isosteric heat of adsorption $q=159\pm6$ meV per CF_4 molecule for coverages close to monolayer completion as determined in Ref. 7 from specular He-reflection experiments. Note that the adsorption energies are only 62% (monolayer) and 64% (bilayer) of the corresponding values for CF_3Cl. This is most likely a consequence of the stronger electrostatic interaction of the CF_3Cl molecules due to their permanent electric dipole moment. Comparison of the temperatures where the monolayer desorption peaks reach their maxima (CF_4, 59.7 K, CF_3Cl, 94.9 K) yields nearly the same ratio (63%).

III. POTENTIAL CALCULATIONS

A. Interaction potential

For the two systems CF_4/Cu(110) and CF_3Cl/Cu(110) the interactions are separated into adsorbate-adsorbate and adsorbate-substrate terms

$$V(\mathbf{R},\mathbf{\Omega})=V_{AA}+V_{AS}. \tag{5}$$

It is assumed that the substrate and the adsorbate are undeformable. $\mathbf{R}(x,y)$ defines the position of the center of mass and $\mathbf{\Omega}(\theta,\varphi,\chi)$ the orientation of the adsorbed molecule (Fig. 4). Note that the local coordinate system is chosen in such a way that the z-molecular axis is along a C-F axis for CF_4, while for CF_3Cl it coincides with the C_3-symmetry axis C-Cl. The origin of this frame is located at the center of mass of the molecule.

The dominant contribution to V_{AA} is the dispersion-repulsion interaction, which is modeled by pairwise atom-atom Lennard-Jones potentials

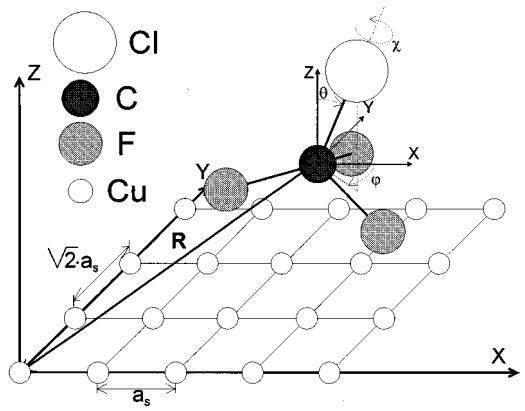

FIG. 4. Adsorption geometry of the pyramidal CF_3Cl molecule on Cu(110). **R** defines the position of the center of mass and (θ,φ,χ) are the Euler angles referred to a frame having its origin at the center of mass of the molecule. For CF_4 the Cl atom is replaced by a F atom and the molecular center of mass coincides with the C nucleus.

$$V_{AA}^{Q}=\sum_{i,j} 4\epsilon_{ij}\left[\left(\frac{\sigma_{ij}}{r_{ij}}\right)^{12}-\left(\frac{\sigma_{ij}}{r_{ij}}\right)^{6}\right]. \tag{6}$$

The sets of parameters (ϵ,σ) are taken from the literature[6,16] and are listed in Table I. To this quantum interaction one must add the multipolar electrostatic potential, which can be represented by interactions between distributed multipolar moments to take into account the finite extension of the electron clouds. The electrostatic interaction in CF_3Cl is modeled by assuming a distribution of charges located at the atomic nuclei.[6] The values are given in Table II. For CF_4, the molecular octupole moment is small and its effect is included through by choosing appropriate ''effective'' values for the Lennnard-Jones parameters, as discussed by Nosé and Klein.[16]

Previously, we have shown that it is possible to describe, to a relatively good accuracy, the interactions between a molecular adsorbate and the (110) face of copper on the basis of simple pairwise potentials. By using combination rules as described in Ref. 10, we have derived Lennard-Jones parameter values for the atomic pairs X-Cu (X=C, F, Cl).

TABLE I. Lennard-Jones parameters for the various pairs of atoms.

Atomic pairs	ε (meV)	σ (Å)
Cu-C[a]	3.36	3.77
Cu-Cl	6.31	3.79
Cu-F[a]	3.29	3.57
C-C[b]	3.32	3.35
C-Cl[c]	8.99	3.30
C-F[b]	3.25	3.15
Cl-Cl[c]	11.70	3.40
Cl-F[c]	5.66	3.17
F-F[b]	3.19	2.95

[a]From Ref. 8.
[b]From Ref. 16.
[c]From Ref. 6.

TABLE II. Charges in electron units located at the corresponding nuclei centers (from Ref. 6).

Charge	(e)
C	0.9486
Cl	−0.1626
F	−0.2620

The potential-energy minimization is performed on the basis of the above potentials, which are known[17,18] to provide the main contribution to the total interaction. Thus, we have disregarded, as a first approximation, the substrate mediated and the polarization interactions, since these terms usually contribute by less than 10% to the adsorption energy and should not change the equilibrium configuration. However, for an accurate evaluation of the adsorption energies and for a comparison with the experimental data, their influence will be taken into account.

B. Potential-energy surfaces for a single admolecule on the substrate

The potential-energy map $V(x,y)$ is obtained by minimizing V_{AS} with respect to z and $\mathbf{\Omega}$. Examination of this map allows us to evaluate the holding potential and the corrugation experienced by a single CF_4 or CF_3Cl molecule, respectively.

1. CF_4

There are two symmetrically equivalent stable sites for CF_4 on Cu(110) [Figs. 5(a) and 5(b)]. These sites are located between two Cu atoms along the [001] direction, at 1.3 Å from the nearest Cu atom. The potential energy at these sites is −163 meV and the molecule adopts a tilted tripod-down orientation, i.e., three F atoms stick to the surface, while the top F atom is tilted by about 20° from the surface normal and points away from the nearest Cu atom along [001].

The corrugation energy, i.e., the amplitude of the lateral variation of the binding energy, is 4 meV along the $[1\bar{1}0]$ direction and 17 meV along the [001] direction. Thus, the molecule preferentially resides inside the potential trough along $[1\bar{1}0]$, with the center of mass (the C atom) being located at 3.70 Å above the surface plane.

2. CF_3Cl

For this adsorbate, there are four symmetrically equivalent sites with an energy of −201 meV [Figs. 5(c) and 5(d)]. At these sites, the molecule lies 3.75 Å above the surface in a tilted tripod-down configuration, the tripod being formed by two F atoms and the Cl atom, with the Cl atom being closest to the surface and pointing towards the center of the rectangular Cu(110) unit cell. This behavior is characteristic for the entire map: the Cl atom, which provides an important contribution to the quantum interaction, is always found in a position where its distances with respect to the neighboring copper atoms are optimized, i.e., close to the center of the substrate unit cell. The corrugation is 5 meV along the $[1\bar{1}0]$ direction and 12 meV along the [001] direction.

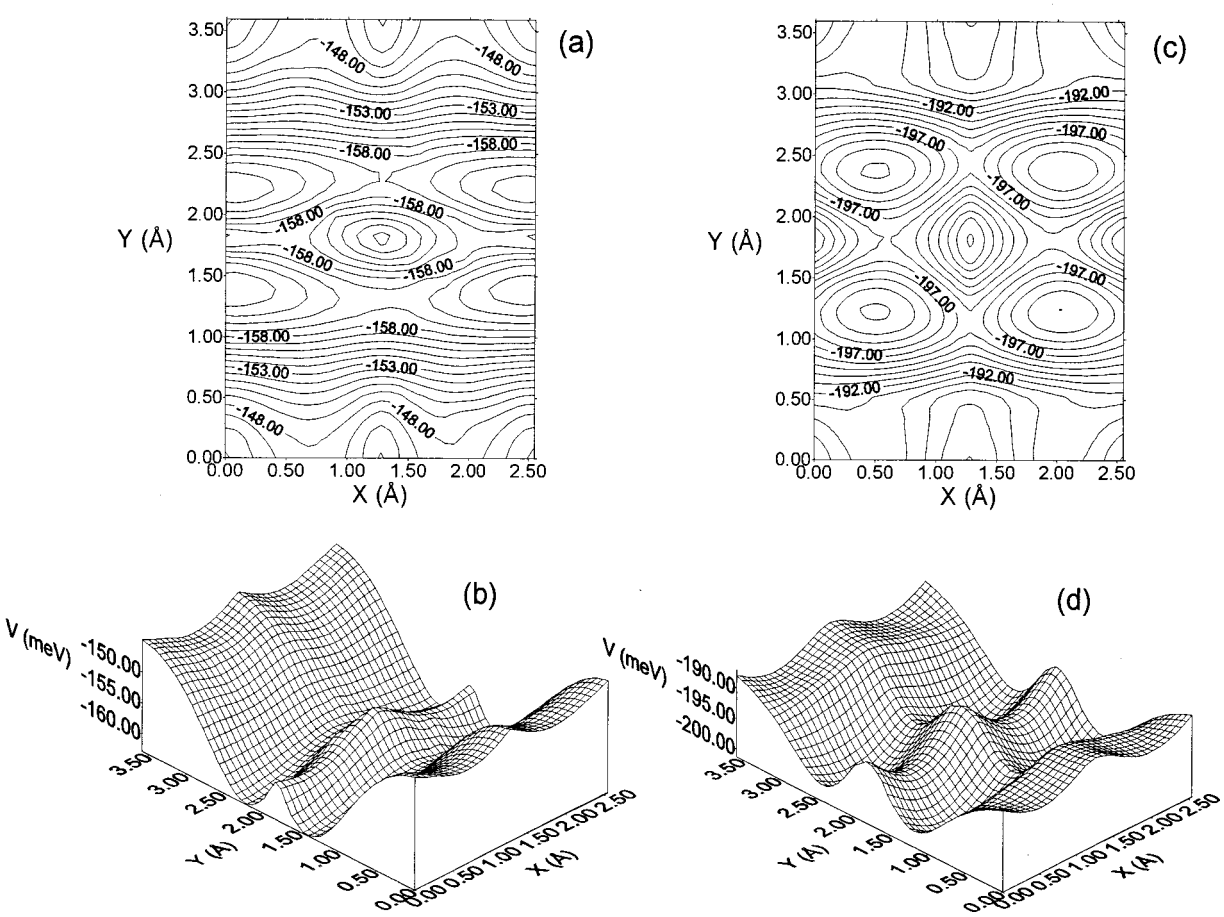

FIG. 5. Potential energy maps for CF_4 [(a) and (b)] and for CF_3Cl [(c) and (d)]. The Cu atoms are located at the corners of the rectangle describing the Cu(110) unit cell.

Except for an overall increase of the binding energy by about 40 meV, the shape of the two maps (CF_4 and CF_3Cl) are very similar, although the equilibrium valleys are less apparent for CF_3Cl and the surface appears smoother. This is a direct consequence of the larger size of the CF_3Cl molecule compared to CF_4.

C. Two-dimensional layers without support

In order to obtain information on the density of the monolayer and on the positions and orientations of the admolecules when lateral interactions are effective, we first perform minimization calculations on the two-dimensional (2D) layers without support. In the lack of information on the orientational ordering in bulk CF_3Cl, we tried an arrangement equivalent to the one we found for the 2D CF_4 layer without support.[8] Then, by relaxing the size of this cell we obtain a rectangular cell with two CF_3Cl molecules, leading to an average area of 17.45 $Å^2$ per molecule and a mean energy of -170 meV. In this cell, the molecular dipoles are oriented in a 2-out herringbone-type pattern. This structure is not very different from the one obtained for CF_4, which is also characterized by a rectangular unit cell, in this case with a mean area of 17 $Å^2$ per molecule and a mean binding energy of -100 meV per molecule.

We recall that the area of the pure copper cell is 9.2 $Å^2$; therefore, the calculated adsorbate density is rather close to one CF_3Cl molecule per two copper unit cells, as is the case for CF_4 (cf. Fig. 5 of Ref. 8).

D. Adsorbed monolayers

Considering the huge size of the experimentally determined $\begin{pmatrix} 17 & 3 \\ 3 & -7 \end{pmatrix}$ superstructure unit cell for $CF_3Cl/Cu(110)$ and the problems related to the potential-energy minimization of monolayers formed by nonlinear molecules,[8] we have limited our discussion to the study of low-commensurate structures.

First of all, we consider the two structures $\begin{pmatrix} 2 & 0 \\ 1 & 1 \end{pmatrix}$ and $\begin{pmatrix} 2 & 1 \\ -1 & 1 \end{pmatrix}$ [cf. Figs. 6(a) and 6(b)], each containing only one CF_3Cl molecule per unit cell, which are compatible with the structure of the 2D layer without support. The results are given in Table III and, surprisingly, lead to the conclusion that the most stable structure is the $\begin{pmatrix} 2 & 1 \\ -1 & 1 \end{pmatrix}$ phase, which corresponds to a density of one molecule per three Cu atoms (i.e., an area of 27.6 $Å^2$ per molecule) and a total energy of -290.9 meV per molecule. This indicates a relatively low packing of admolecules, which is clearly in contradiction with the CF_4 case, where the most stable structure is obtained for the $\begin{pmatrix} 2 & 0 \\ 1 & 1 \end{pmatrix}$ phase with cell area equal to 18.4 $Å^2$ containing one molecule of energy -232.5 meV [Fig. 6(a)].

However, it is possible to achieve more stable structures when we consider cells containing two molecules. We allow the two molecules to move and orient independently above the surface. The $\begin{pmatrix} 2 & 1 \\ -2 & 2 \end{pmatrix}$ phase with two molecules is exactly twice the size of the primitive $\begin{pmatrix} 2 & 1 \\ -1 & 1 \end{pmatrix}$ unit cell described above. The arrangement of the molecules turns out to be identical to the one in the primitive cell. The two molecules

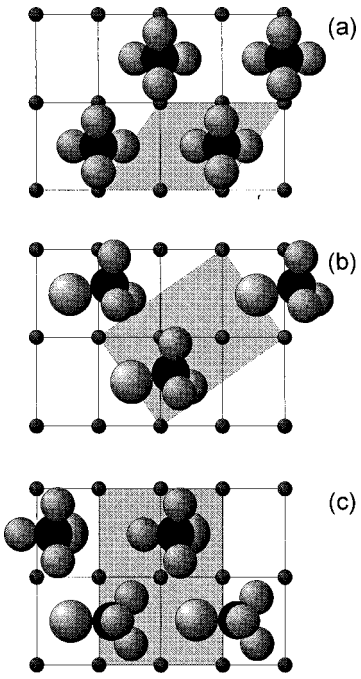

FIG. 6. Geometries of stable low-order commensurate structures considered in Table III; (a) $\begin{pmatrix} 2 & 0 \\ 1 & 1 \end{pmatrix}$ phase for CF_4, (b) $\begin{pmatrix} 2 & 1 \\ -1 & 1 \end{pmatrix}$ phase for CF_3Cl, (c) $\begin{pmatrix} 2 & 0 \\ 0 & 2 \end{pmatrix}$ or (2×2) for CF_3Cl. The corresponding unit cells are indicated by the dark areas.

are thus equivalent with an energy per molecule equal to -290.9 meV. A truly new and more stable structure is obtained for the (2×2) phase with a $\begin{pmatrix} 2 & 0 \\ 0 & 2 \end{pmatrix}$ unit cell, with an area per molecule equal to 18.4 $Å^2$ and a mean energy of -297.6 meV per molecule. This phase displays interesting new features. Most noticeable of all is its bilayer structure since it contains two nonequivalent molecules at different heights above the surface. The binding energy of the upper molecule is -267.8 meV, whereas for the lower it is -321.4 meV. It can be noted that the two most stable phases, though very different with respect to their density, lead to very similar binding energies. Moreover, Figs. 6(b) and 6(c) show that in the first case, the molecular axes are all oriented in the same direction parallel to the Cu troughs, resulting in ''ferroelectric'' dipolar ordering, whereas in the (2×2) phase the dipoles are arranged almost antiparallel. The molecular density appears clearly too low in order to optimize the lateral interactions in Fig. 6(b), whereas it is too large in Fig. 6(c) to allow complete molecular reorientation.

It is likely that the absolute energy minimum has not been reached for the (2×2) phase and that unit cells containing more than two molecules could lead to even more stable structures. The experimentally observed $\begin{pmatrix} 13 & -7 \\ 3 & 3 \end{pmatrix}$ superstructure, however, clearly contains such a large number of molecules per unit cell, which does not allow us to perform an accurate numerical minimization for this structure in reasonable computing time.

The fact that the surface is smoother for CF_3Cl than for CF_4 may explain the instability of the $\begin{pmatrix} 2 & 0 \\ 1 & 1 \end{pmatrix}$ low-order commensurate phase for CF_3Cl. Such a behavior is consistent with the He-diffraction experiments, which reveal completely different structures for the two systems. Anyway, the calculated binding energies provide a good estimate of the adsorption energy per molecule for the CF_3Cl monolayer on Cu(110). Indeed, it has been shown for CF_4 (and also been verified for CF_3Cl) that a refined search for the most stable structure by including larger and larger unit cells, generally leads to orientational and positional changes of the admolecules but does not dramatically decrease the binding energy per molecule. Since we are more interested here in an estimate of the adsorption energy we will rather focus on the precise evaluation of the adsorption energy for the most stable low-order commensurate structure and its comparison with the experiment.

E. Thermodynamics

A direct comparison with the adsorption energy measured in a thermal desorption experiment requires us to account for energy corrections to the potential values calculated in Sec. III D. First of all, we add to the minimum potential value V the substrate mediated interaction and the surface induced dipole-dipole interaction. The origin and approximate size of these two terms which describe the molecule polarization by the substrate have been discussed for CF_4 in Ref. 8. They contribute with about 3 meV and about 12 meV, respectively, to the total binding energy per molecule. We may assume that similar numbers also hold for CF_3Cl. Note that these corrections are repulsive and tend to reduce the poten-

TABLE III. Equilibrium configurations (in Å, deg.) and potential-energy values (in meV) of the molecules in various adlayer configurations.

N[a]	Cell[a]	A[b]	x	y	z	θ	φ	χ	V_{AA}	V_{AS}	$\overline{V}$
1[c]	$\begin{pmatrix} 2 & 0 \\ 1 & 1 \end{pmatrix}$	18.39	1.71	1.02	4.72	149	118	62	−130.0	−140.1	−270.1
1[c]	$\begin{pmatrix} 2 & 1 \\ -1 & 1 \end{pmatrix}$	27.59	0.48	2.12	3.82	106	187	144	−99.0	−191.9	−290.9
2[c]	$\begin{pmatrix} 2 & 0 \\ 0 & 2 \end{pmatrix}$	18.39	0.47 2.91	1.71 5.32	3.90 4.87	113 160	180 0	60 0	−136.6 −136.6	−190.8 −131.2	−297.6
2[c]	$\begin{pmatrix} 2 & 1 \\ -2 & 2 \end{pmatrix}$	27.59	0.48 −2.07	2.12 5.92	3.82 3.82	106 106	187 187	144 144	−99.0 −99.0	−191.9 −191.9	−290.9
1[d]	$\begin{pmatrix} 2 & 1 \\ 1 & 1 \end{pmatrix}$	18.39	0.00	1.81	3.70	0	0	90	−82.5	−150.1	−232.5

[a]N denotes the number of molecules in the cell defined by the indicated square matrix.
[b]Mean area per molecule in the adlayer, in $Å^2$.
[c]CF_3Cl monolayer.
[d]CF_4 monolayer.

TABLE IV. Harmonic frequencies ω_α (meV) for the molecules in the most stable adlayers.

α	CF_4	CF_3Cl
x	3.70	3.15
y	2.49	3.49
z	2.73	2.90
θ	2.10	3.05
φ	3.20	6.55
χ	3.90	5.50

tial depth at equilibrium by about 15 meV per molecule for the CF_4 and CF_3Cl monolayers.

A second correction arises from the finite temperature contribution. Indeed, the adsorption/desorption energy per molecule can be written as[19]

$$E_A = -V + 15\text{meV} + k_B T \sum_{\alpha=1}^{6} \left(\frac{1}{2} - \frac{\hbar\omega_\alpha}{2k_B T} \coth \frac{\hbar\omega_\alpha}{2k_B T} \right), \tag{7}$$

where the dynamical contribution originates from the oscillatory motion for the various translational ($\alpha = x,y,z$) and rotational ($\alpha = \theta,\varphi,\chi$) degrees of freedom of the admolecule in the monolayer. We have assumed that all these motions can be approximated by harmonic oscillators with frequencies ω_α. These frequencies, listed in Table IV, have been calculated for the most stable structures of CF_4 and CF_3Cl given in Table III by determining the harmonic force constants k_α and the corresponding mass ($\alpha = x,y,z$) or moment of inertia ($\alpha = \theta,\varphi,\chi$) for the different motions, which are assumed to be decoupled.

The frequencies all lie below 6 meV ($\simeq 50$ cm^{-1}) for the various motions of the two inequivalent molecules, leading to a temperature dependent correction in Eq. (7) equal to 17 meV at around 60 K. The resulting values of the adsorption energy E_A are thus 200 meV for CF_4 and 266 meV for CF_3Cl.

IV. COMPARISON WITH EXPERIMENTS AND DISCUSSION

In contrast to the CF_4 monolayer for which the energy optimization procedure was applied to relatively large unit cells (2×18 structure) containing 18 molecules, we have limited this procedure to low-order commensurate phases for CF_3Cl. Indeed, given the size of the $\begin{pmatrix} 13 & -7 \\ 3 & 3 \end{pmatrix}$ unit cell deduced from the diffraction pattern, the number of molecules per unit cell should range between 25 and 30. The large number of degrees of freedom prevented any serious analysis of the adlayer geometry from energy minimization calculations. However, the results obtained for the simple unit cells show trends, which can be discussed and compared to the behavior of CF_4. In the CF_4 monolayer, one molecule occupies a mean area of 18.4 Å^2 with a lateral energy representing only 35% of the total binding energy. The same unit cell used for CF_3Cl would lead to a structure for which the lateral energy takes nearly the same value as the holding contribution. This is not surprising regarding the polar nature of the pyramidal molecule. The dipolar lateral contribution is responsible for the large reorientation of the two molecules when we consider a unit cell with twice the previous area. On one hand, we see from Table III that the lateral interactions tend to be optimized whereas the holding interactions are very different for the two molecules. This indicates that the molecules would prefer to adopt a configuration where their dipoles are antiparallel, thus giving rise to an arrangement of dipolar chains along the Cu troughs with antiferroelectric ordering between adjacent chains. On the other hand, the values of the holding energies of the two inequivalent molecules are quite different. This suggests that the two molecules might prefer to increase their mutual distance along the Cu trough to reduce the compression on the surface. As a result, the unit cell would significantly increase to recover registry with the substrate, in agreement with the large unit cell obtained in diffraction experiments. This feature is corroborated by examination of the dipolar arrangements in Figs. 6(b) and 6(c). The actual density is probably intermediate between the two drawn structures, leading to high-order commensurate phases. The tendency to form antiparallel ferroelectric chains for CF_3Cl on Cu(110) is consistent with the observation of a high-order commensurate phase with a similar stacking sequence of ferroelectric chains on the (0001) plane of exfoliated graphite.[5]

When we compare the calculated values of E_A with the monolayer adsorption energies determined from the TDS spectra (Sec. II B), we find a very good agreement for CF_3Cl: the theoretical value is overestimated by less than 5%, whereas the calculation yields a value for CF_4 which is 20% too large. There can be several reasons for such a difference in accuracy. For CF_4, the adsorption energy has been calculated for the structure, which seems to be reasonably close to the minimum energy configuration. The numerical efforts devoted previously[8] to determine the correct structure for CF_4 adsorbed on Cu(110) seem to justify that, in this case, the calculated adsorption energy is quite close to the minimum value. In contrast, for CF_3Cl, only reasonably small sizes for the unit cell have been considered in the minimization calculation, and we are not sure that we have reached the absolute minimum for CF_3Cl on Cu(110). As a consequence, the theoretical adsorption energy for CF_3Cl could be larger than the present value of 297.6 meV. However, as already mentioned, the minimum energy is not so sensitive to a small reorientation and relocation of the molecules required for a correct description of the adlayer structure, and we trust that our present value of E_A is rather close to the value, which would be reached at the absolute minimum.

Another cause could be the overestimation of the parameters connected to the holding potential. Indeed, the combination rules used to estimate the Lennard-Jones parameters for the pairs Cu-X (X=C, F, Cl) are known to be only approximate and their extrapolation from the Xe-Cu and N_2-Cu pairs to other species may be questionable. For instance, decreasing the $\epsilon_{\text{Cu-}X}$ parameter by 10% would reduce the holding potential V_{AS} for CF_4 and CF_3Cl by the same factor leading to values for V_{AS} equal to -135 meV for CF_4 and -145 meV for CF_3Cl. The lateral interaction would not be affected and, as a result, the binding energy would be reduced by about 17 meV leading to final E_A values of 183

meV for CF_4 and 250 meV for CF_3Cl, in reasonable agreement with the experimental data.

To go beyond, we use our potential to determine the interaction energy per molecule in the CF_4 and CF_3Cl bulk crystals. The calculated values at 0 K are -200 meV for CF_4, in obvious agreement with the result of Nosé and Klein[16] since we adopted the same potential parameters, and -280 meV for CF_3Cl. If we estimate that the kinetic energy increases these values by about 30 meV at 70 K, the calculated heats of adsorption are equal to 170 meV for CF_4 and 250 meV for CF_3Cl. These values are in reasonable agreement with the present TDS measurements, yielding multilayer desorption energies of 150 meV and 204 meV, respectively. They can furthermore be compared to the value of the measured heat of condensation for the CF_4 monolayer adsorbed on graphite at 70–100 K (Ref. 20), which ranges between 196 and 215 meV and to the heat of multilayer CF_4 sublimation equal to 174 meV at 70 K.[21].

In conclusion, semiempirical potential calculations applied to CF_4 and CF_3Cl monolayers adsorbed on the Cu(110) surface give a good account of the adsorption energy per molecule when compared to thermal desorption experiments. It seems a rather general feature that simple empirical potentials applied to molecular adsorbates (Ar, Xe, N_2, CO, CH_4) on metals can yield accurate adsorption energies, layer structure, and phase transition, and even, in some specific situations [for instance, Xe on Cu(110)], consistent phonon dispersion relations. For simple monatomic or diatomic species, the layer structures are either low-order commensurate phases implying a small number of degrees of freedom, or incommensurate phases if the lateral interactions are much stronger than the substrate corrugation. Under these circumstances, the numerical search of the layer geometry appears to be quite accurate. In contrast, when the corrugation is not negligible or/and the unit cell contains a large number of molecules, the numerical procedures are not accurate enough to unambiguously determine the structure of these monolayers and only trends can be established in conjunction with diffraction data. In the present case, we may expect that in the light of the experimental data and the calculations, the strong dipolar nature of the pyramidal CF_3Cl molecule could give rise to the formation of antiparallel (ferroelectrically) ordered chains on Cu(110), as already discussed for CF_3Cl on graphite.

ACKNOWLEDGMENTS

We thank H. Zeng-Martel for help in setting up the thermal desorption spectrometer. We also gratefully acknowledge the support of this work by a grant from the Deutscher Akademischer Austauschdienst (DAAD) and the Ministère des Affaires Etrangères (MAE) via the PROCOPE program.

*Present address: Institut für Experimentalphysik, Johannes-Kepler-Universität Linz, Altenbergerstr. 69, 4040 Linz, Austria.

[1] L. W. Bruch, M. W. Cole, and E. Zaremba, *Physical Adsorption: Forces and Phenomena* (Clarendon, Oxford, 1997).
[2] L. W. Bruch, J. Chem. Phys. **87**, 5518 (1987).
[3] T. Kawai and N. Nakamura, J. Chem. Phys. **103**, 3755 (1995).
[4] K. Kjaer, M. Nielsen, J. Bohr, H. J. Lauter, and J. P. Mc Tague, Phys. Rev. B **26**, 5168 (1982).
[5] W. Weimer, K. Knorr, and H. Wiechert, Phys. Rev. Lett. **61**, 1623 (1988).
[6] W. R. Hammond and S. Mahanti, Surf. Sci. **234**, 308 (1990).
[7] V. Diercks, J. Goerge, P. Zeppenfeld, R. David, and G. Comsa, Surf. Sci. **352–354**, 274 (1996).
[8] A. Marmier, P. N. M. Hoang, C. Ramseyer, C. Girardet, V. Diercks, and P. Zeppenfeld, J. Chem. Phys. **107**, 653 (1997).
[9] C. Ramseyer, C. Girardet, P. Zeppenfeld, J. Goerge, M. Büchel, and G. Comsa, Surf. Sci. **313**, 251 (1994).
[10] P. Zeppenfeld, J. Goerge, V. Diercks, R. Halmer, R. David, G. Comsa, A. Marmier, C. Ramseyer, and C. Girardet, Phys. Rev. Lett. **78**, 1504 (1997); A. Marmier, C. Ramseyer, P. N. M. Hoang, C. Girardet, J. Goerge, P. Zeppenfeld, M. Büchel, R. David, and G. Comsa, Surf. Sci. **383**, 321 (1997).
[11] R. David, K. Kern, P. Zeppenfeld, and G. Comsa, Rev. Sci. Instrum. **57**, 2771 (1986).
[12] P. Zeppenfeld, M. Büchel, J. Goerge, R. David, G. Comsa, C. Ramseyer, and C. Girardet, Surf. Sci. **366**, 1 (1996).
[13] H. Schlichting and D. Menzel, Surf. Sci. **272**, 27 (1992); H. Schlichting, Ph.D. thesis, TU Munich (1990).
[14] G. Ehrlich, Appl. Phys. Lett. **32**, 4 (1961).
[15] H. J. Kreuzer and Z. W. Gortel, *Physisorption Kinetics*, Springer Series in Surface Sciences Vol. 1 (Springer, Berlin, 1986).
[16] S. Nosé and M. L. Klein, J. Chem. Phys. **78**, 6928 (1983).
[17] W. Steele, Chem. Rev. **93**, 2355 (1993).
[18] L. W. Bruch, Surf. Sci. **125**, 194 (1983).
[19] A. Lakhlifi and C. Girardet, Surf. Sci. **214**, 400 (1991).
[20] P. Dolle, M. Matecki, and A. Thomy, Surf. Sci. **91**, 271 (1980).
[21] B. Genot and X. Duval, J. Chim. Phys. Phys.-Chim. Biol. **67**, 1332 (1970).